Improved Starlink Satellite Orbit Prediction via Machine Learning with Application to Opportunistic LEO PNT

Paul El Kouba, Samer Hayek, Joe Saroufim, and Zaher M. Kassas *The Ohio State University*
Evan Fakhoury, *Lebanese American University*

BIOGRAPHY

Paul El Kouba is a Ph.D. student in the Department of Electrical and Computer Engineering at The Ohio State University and a member of the Autonomous Systems Perception, Intelligence, and Navigation (ASPIN) Laboratory. He received a B.E. in Computer Engineering from the Lebanese American University. His research interests include low Earth orbit (LEO) satellites, satellite-based navigation, cognitive software-defined radio, and machine learning.

Samer Hayek is a Ph.D. student in the Department of Electrical and Computer Engineering at The Ohio State University and a member of the ASPIN Laboratory. He received a B.E. in Mechanical Engineering from the Lebanese American University. His research interests include LEO satellites, autonomous vehicles, sensor fusion, and simultaneous localization and mapping.

Joe Saroufim s a Ph.D. student in the Department of Electrical and Computer Engineering at The Ohio State University and a member of the ASPIN Laboratory. He received a B.E. in Mechanical Engineering from the Lebanese American University. His research interests include LEO satellites, situational awareness, autonomous vehicles, and sensor fusion.

Evan Fakhoury earned his Master's of Science in Advanced Mechanical Engineering from the University of Leeds in 2011, followed by his PhD in 2016 in Mechanical Engineering, specializing in Human-Computer Interaction. He currently serves as an Assistant Professor of Mechanical Engineering and the Assistant Director of the Industrial Hub at the Lebanese American University. His research centers on advanced applications of virtual and augmented reality technologies to address real-world challenges, with a particular focus on education, manufacturing, navigation, simulation, and training. Dr. Fakhoury's work aims to bridge innovative technology with practical problem-solving across multiple industries.

Zaher (Zak) M. Kassas is the TRC Endowed Chair in Intelligent Transportation Systems (ITS), a professor at The Ohio State University, Director of the ASPIN Laboratory, and Director of the U.S. Department of Transportation Center: CARMEN (Center for Automated Vehicle Research with Multimodal AssurEd Navigation), focusing on navigation resiliency and security of highly automated transportation systems. He received a B.E. with Honors in Electrical Engineering from the Lebanese American University, an M.S. in Electrical and Computer Engineering from The Ohio State University, and an M.S.E. in Aerospace Engineering and a Ph.D. in Electrical and Computer Engineering from The University of Texas at Austin. He is a recipient of the National Science Foundation (NSF) CAREER award, Office of Naval Research (ONR) Young Investigator Program (YIP) award, Air Force Office of Scientific Research (AFOSR) YIP award, IEEE Walter Fried Award, IEEE Harry Rowe Mimno Award, Institute of Navigation (ION) Samuel Burka Award, and ION Col. Thomas Thurlow Award. He is a Fellow of the IEEE and the ION and a Distinguished Lecturer of IEEE Aerospace and Electronic Systems Society and IEEE Intelligent Transportations Systems Society. His current research interests include navigation systems, LEO satellites, cognitive sensing, and ITS.

ABSTRACT

A machine learning (ML) framework for improved Starlink low Earth orbit (LEO) satellites' orbit prediction is presented. The framework exploits newly published SpaceX ephemerides files containing relatively low errors during the first eight hours of release. This framework assumes two stages: (i) data processing stage that uses the published SpaceX ephemerides files to learn the error between the given data and propagated ephemerides using the simplified general perturbations (SGP4) model, which are subsequently used to train a time-delay neural network (TDNN); and (ii) forecasting stage over a certain period of time where the errors are estimated to correct the SGP4-propagated orbits. Simulation results are presented showing that the ML approach achieved mean satellite position and velocity errors of 177 m and 0.86 m/s, respectively. In contrast, the SGP4-propagated ephemerides' mean position and velocity errors were 2,535 m and 2.75 m/s, respectively. An unknown receiver could use the forecasted TDNN-improved Starlink ephemerides to localize itself using Doppler measurements from overhead Starlink satellites. Simulation results are presented to showcase the improvement in stationary receiver localization upon relying on the TDNN-improved Starlink ephemerides. Fusing Doppler measurements from 19 Starlink satellites over a 5-minute period via an extended Kalman filter, if a stationary receiver is to rely on SGP4-propagated orbits to localize itself, an initial position error of 6.5 km gets reduced to 2.3 km, whereas the TDNN-corrected ephemerides reduces the position error to 53 m.

Preprint of the 2024 ION GNSS+ Conference Baltimore, Maryland, September 16–20, 2024

I. INTRODUCTION

Over the past few years, the world has observed a surge in low Earth orbit (LEO) satellites typically stationed between 160 and 2,000 km above the Earth's surface. This drastic increase in LEO satellites has resulted in more than 6,700 active satellites orbiting the Earth as of 2024 (Union of Concerned Scientists, 2024). In fact, SpaceX has contributed to more than 5,500 Starlink satellites and is planning to launch thousands more in the foreseeable future (Gal and Talbi, 2024).

This increase in LEO satellites has resulted in a massive global network coverage, aimed generally for wireless communications. Despite being designed for communications, LEO satellites' signals can be used opportunistically for positioning, navigation, and timing (PNT) applications (Kassas et al., 2021; Jardak and Jault, 2022; Hartnett, 2022; Kassas et al., 2023b; Stock et al., 2024; Fan et al., 2024; Liu et al., 2024; Kassas et al., 2024b; Zhao et al., 2023; Prol et al., 2024). LEO satellites' proximity to Earth grants higher received signal power (Reid et al., 2021; Kozhaya et al., 2024). In addition, LEO satellites transmit in a wide swath of the spectrum (e.g., Orbcomm transmits in the VHF-band, Iridium in the L-band, and Starlink and OneWeb in the Ku-band) (Kassas et al., 2023a). These make LEO-based PNT more resilient to unintentional interference, jamming, and malicious spoofing (Burbank et al., 2024).

Exploiting LEO signals of opportunity for PNT comes with three challenges: (i) designing specialized receivers to extract navigation observables; (ii) compensating for the satellites' unknown clock errors; and (iii) estimating the satellites' ephemerides to the highest accuracy possible. Existing literature has been tackling the first two challenges, with many studies proposing receiver designs to properly extract the navigation observables: pseudorange, carrier phase, and/or Doppler (Khalife and Kassas, 2019; Tan et al., 2019; Farhangian and Landry, 2020; Khalife et al., 2022; Huang et al., 2022; Jardak and Adam, 2023; Kozhaya et al., 2023; Grayver et al., 2024; Xie et al., 2024b; Shahcheraghi and Kassas, 2024), while other studies considered the analysis and estimation of clock errors (Ye et al., 2023; El-Mowafy et al., 2023; Gosalia et al., 2023; Xie et al., 2024a; Wang et al., 2024). This paper tackles the ephemeris estimation challenge.

Satellite orbit propagator models have been developed in the literature (Montenbruck and Gill, 2000; Schutz et al., 2004). These models differ in time complexity and accuracy. The most basic method to propagate a satellite is by mathematically solving the satellite's second order differential equation using an unperturbed Kepler orbit. However, this model leads to highly inaccurate results since there are multiple forces that affect the satellite. To alleviate this, one could employ numerical and analytical models that take into consideration these forces (i.e., atmospheric drag, gravity, etc.) to capture the different perturbations affecting the satellite.

One common numerical propagator is the two-body model with J_2 perturbations that takes into consideration the J_2 effect as the major contributing perturbation, based on Earth's oblateness (Morales et al., 2019). A more accurate numerical propagator is the high-precision orbit propagator (HPOP) that can yield highly accurate results if initialized properly. However, HPOP requires force model parameters that might not be available or reliable for non-cooperative LEO. Additionally, calculating all the forces acting on the satellites is a computationally heavy task that would consume a lot of time; deeming them unfit for real-time applications (Imre and Palmer, 2007).

On the other hand, analytical approaches like the simplified perturbation models (e.g., SGP4 and SDP4) can be used for orbit estimation. These models are usually initialized by the satellites' Keplerian elements, also known as classical orbital elements, found in two-line elements (TLE) files publicly published by the North American Aerospace Defense Command (NORAD) on a daily basis (North American Aerospace Defense Command (NORAD), 2018). They can estimate the satellites' positions faster, but at the compromise of accuracy. For example, the SGP4 model initialized with Keplerian elements from satellites' TLE files does not reach desirable accuracy due to initial errors reaching almost 2.5 km (Khairallah and Kassas, 2021; Stock et al., 2024). Since NORAD updates TLE files on a daily basis, propagation models might start their estimates minutes after the TLE file is uploaded, or hours later, which would induce propagation errors. Additionally, to obtain ephemeris sets, TLE files have to be propagated for several hours which accumulates position and velocity errors.

After the boom in artificial intelligence (AI) and machine learning (ML) advancements in the late 2010s, researchers started looking into ML approaches to estimate and propagate satellites' orbits. In (Sharma and Cutler, 2015; Feng et al., 2019), distribution regression was used for orbit determination of objects in LEO. Propagating LEO satellite orbits was studied in (Peng and Bai, 2017, 2018) via neural networks (NNs), support vector machines (SVMs), and Gaussian processes (GPs). A simulation study developed in (Peng and Bai, 2018, 2019) showed that NNs possess high regression capabilities compared to SVMs and GPs. Several NN architectures, such as time-delay NN (TDNN) and long short-term memory (LSTM) NNs were studied in (Salleh et al., 2019). ML's powerful capabilities have been recently studied to provide a less parameter-reliant orbit propagation solution (Wang et al., 2021; Shen et al., 2021). ML for LEO orbit propagation with application to PNT has been considered in (Mortlock and Kassas, 2021; Kozhaya et al., 2021).

A promising recent study proposed a closed-loop, three-parts framework that exploits two overhead passes of LEO satellites and uses a TDNN model to propagate the orbits (Haidar-Ahmad et al., 2022; Kassas et al., 2024a). During the first pass, a known receiver in a known location tracks visible satellites overhead and gets their ephemerides using a two-body propagation model with $J2$. After the satellite becomes out-of-sight, the tracked ephemerides are used as inputs to a TDNN model with SGP4-propagated data as an exogenous input to stabilize the network and help it better estimate the nonlinear orbit. Finally, once the satellite is back in view, the predicted data from the TDNN model are used to localize an unknown receiver.

Recently, SpaceX started uploading Starlink ephemerides publicly in a modified ITC format (Starlink, 2024). Each file is uploaded every 8 hours and is deleted after 24 hours of its publication. Additionally, the uploaded files contain a satellite's three-dimensional (3D) position and velocity in the Earth-centered inertial (ECI) frame and the covariance errors in the radial, in-track, and cross-track (UVW) frame, propagated over 72 hours after the upload time. Over the first 8 hours, it is possible to use the ephemerides for PNT since the covariance errors are relatively low; however, after that time, this error increases drastically, and the data becomes unreliable.

This research introduces a two-part framework that exploits the accuracy of the Starlink uploaded ephemerides: (i) a training phase where a TDNN is trained on predicting the error between the SpaceX ephemerides and an SGP4 propagator and (ii) a forecasting phase where the error is predicted over a certain period of time to correct the SGP4-propagated orbits. To validate the error forecasting and SGP4 correction, an uploaded SpaceX file was kept from training and was used as ground truth testing data. Simulation results are presented showing that the ML approach achieved mean satellite position and velocity errors of 177 m and 0.86 m/s, respectively. In contrast, the SGP4-propagated ephemerides' mean position and velocity errors were 2,535 m and 2.75 m/s, respectively. An unknown receiver could use the forecasted TDNN-improved Starlink ephemerides to localize itself using Doppler measurements from overhead Starlink satellites. Simulation results are presented to showcase the improvement in stationary receiver localization upon relying on the TDNN-improved Starlink ephemerides. Fusing Doppler measurements from 19 Starlink satellites over a 5-minute period via an extended Kalman filter (EKF), if a stationary receiver is to rely on SGP4-propagated orbits to localize itself, an initial position error of 6.5 km gets reduced to 2.3 km, whereas the TDNN-corrected ephemerides reduces the position error to 53 m.

This paper is organized as follows. Section II describes the considered problem. Section III discusses the data collection and outlines the proposed ML framework. Section IV provides simulation results. Section V presents concluding remarks.

II. PROBLEM DESCRIPTION

Having the ephemerides of Starlink satellites published three times per day with low covariance values over the non-overlapping time frames provides accurate ephemerides sets that could be attractive for PNT. However, SpaceX sometimes misses one or multiple consecutive files upload which would lead to periods with relatively uncertain or unavailable ephemeris information.

In such cases, reverting back to previous ML approaches like the two-pass framework introduced in (Haidar-Ahmad et al., 2022; Kassas et al., 2024a) could be problematic, since Starlink satellites might not be transmitting towards a given receiver (Kozhaya et al., 2024). Missing a satellite pass would increase the receiver's localization uncertainty since the ML model would have to estimate the satellite's orbits for a longer of period.

The proposed framework remedies both aforementioned problems. The proposed solution is divided into two phases:

1. **Training Phase:** where the error difference between ephemerides obtained from an SGP4 propagator, initialized with TLE files, and the SpaceX-uploaded ephemerides files is used to train a TDNN ML model.
2. **Forecasting Phase:** where the previously trained TDNN model is used to forecast the error, which is subsequently used to correct SGP4-estimated ephemerides.

III. PROPOSED FRAMEWORK

This section discusses the proposed ML-based framework that utilizes SpaceX-published ephemerides. The training phase consists of two steps: data preparation and training of the ML model. After training is complete, the second phase starts where the previously trained model is used to forecast and correct the SGP4 propagation. Figure 1 summarizes the two phases. The following subsections discuss the data processing step, the ML model, and the forecasting solution.

1. Data Preparation

In every machine learning problem, the most crucial part is proper data collection and preparation on which the model is trained. If done incorrectly, the model would generate false and/or inaccurate outputs. In this paper, the data preparation is twofold: (i) getting the satellites' positions and velocities using both the published ephemerides files (considered as ground truth) and SGP4-propagated ephemerides and (ii) finding the error difference between both orbits.

For open-loop orbit forecasting, it is unadvised to train on the satellites positions and velocities directly since the ML model will not be able to properly predict the different forces that might affect the satellites at any time. Thus, training on and predicting the errors between two propagators would cancel the forces effects since both propagators already took them into account and

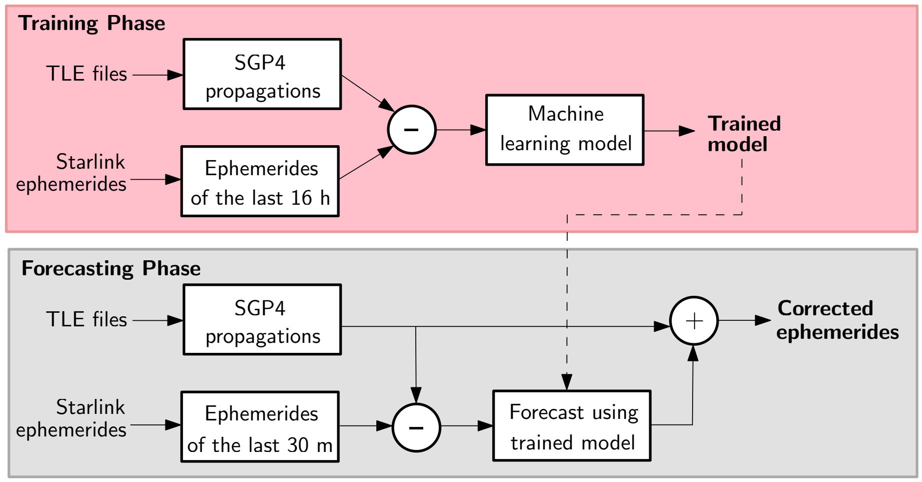

Figure 1: Architecture of the proposed framework

what is being estimated now is only the difference in behaviors between two models, which could be less nonlinear.

To collect and process the data, the last 2–3 ephemerides files published by SpaceX are retrieved and processed to isolate the first 8 hours of each one, resulting in 16 to 24 hours of propagated data. For the SGP4 data, the most recent TLE files are retrieved and the model propagates the satellites over the same period of time as the data given by the ephemerides files. After getting the satellites' positions and velocities from both ephemerides files and SGP4 propagator, they are subtracted to get the error difference between the ground truth and the SGP4-propagated ephemerides which will be the input to the ML model.

2. Machine Learning Model

Once the data is collected and processed, it is fed into an ML model for training. The model's architecture is discussed next.

The problem at hand can be considered a time-series forecasting problem where the model can use the previous estimates to predict the next steps. For time-series forecasting, the literature usually implemented deep learning models (e.g., LSTM) or generative models (e.g., generative adversarial network (GAN), variational autoencoder (VAE), transformers) (Zeroual et al., 2020). However, such models require a large amount of data in order to properly train and predict (Lee and Park, 2019). The SpaceX ephemerides provide around 960 data points to train on, which is not enough for deep models.

Taking into consideration the limited training data, a smaller TDNN model was considered. This model, shown in Figure 2, differs from the typical multilayer perceptron (MLP) TDNN by adding a convolutional layer right after the inputs in order to extract additional features and find dependencies in time between the data points. After convolving the inputs, a maxpooling and a flattening layers are added to change the dimensions of the weight before proceeding with dense layers that will give the outputs.

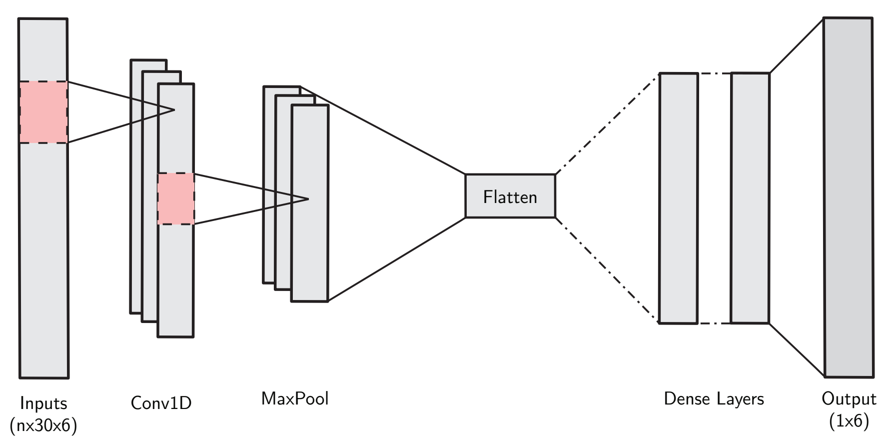

Figure 2: Architecture of the TDNN model

Once the architecture is defined, the hyper-parameters must be tuned. This step allows the model to learn how to generalize over longer periods of time instead of overfitting and memorizing the training-set's behavior and replicating it for the output. For this task, a search space shown in Table 1 was introduced with different parameters that are tuned to optimize the forecasting results. Out of all these parameters, the final model used ReLU as an activation function, Adam as optimizer, and 30 data samples as input in the TDNN.

Table 1: Hyper-parameters Search Space

Parameter	Value
Activation Function	Linear, ReLU, sigmoid, tanh
Optimizer	Adam, SGD, Adagrad
Number of Inputs	[5, 10, 30, 60]

3. Forecasting and Correction of the Orbit

The second phase of the framework starts with another data processing step very similar to that discussed in Section III.1. It starts by downloading the last published ephemerides file from SpaceX and isolating the last 30 minutes of the first 8 hours to get the ML input data. Then, SGP4 is used to propagate the most recent TLE file at the time of the study to calculate the error difference between both ephemeris sets.

After obtaining the input data, the TDNN is used to forecast the errors and add them to the SGP4-propagated orbits to obtain corrected ephemerides for the satellite that could be used for PNT. One should note that the time samples between the data samples from the SGP4 propagator and the outputs from the TDNN need to be uniformly sampled in order to correct the orbital positions and velocities; otherwise, the error would increase instead of attenuate.

Additionally, after the ML model forecasts the correction errors for the satellites' 3D position and velocity at the next time-step, this new output will be used as an input by replacing the oldest data sample there. With this recursive loop, the TDNN would be able to correct the ephemerides for a long period of time.

IV. SIMULATION

This section evaluates the performance of the proposed framework through a receiver localization simulation. Here, a stationary, Earth-based receiver's position will be estimated using: (i) ground truth data (satellites' ephemerides published by SpaceX), (ii) TLE and SGP4 data, and (iii) corrected SGP4 data using the TDNN proposed in the previous section.

1. Simulation Setup

To start the simulation, all Starlink satellites' TLE files were retrieved and propagated using SGP4 in order to have a position and velocity time series estimate of each one. This was done to check which satellites are visible over Columbus, Ohio, USA, where the receiver will be localized in the simulation. Over a period of 5 minutes: from 11:16 until 11:21 on September 6th, 2024, 19 visible Starlink satellites were selected whose trajectories are plotted in the skyplot in Figure 3.

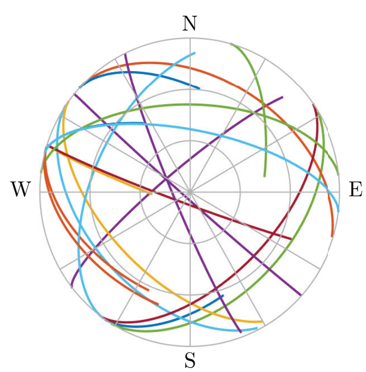

Figure 3: Skyplot of the 19 Starlink satellites considered in the simulation study

For this simulation, the training data started 16 hours before and stopped 1 hour before these 19 satellites are visible leaving a 1 hour forecast duration. The difference between the ground truth position and velocity of these 19 satellites and their SGP4 propagation and between the ground truth and the TDNN forecast correction are plotted in Figure 4.

The mean position and velocity errors for both SGP4 and ML approaches during the last 5 minutes are tabulated in Table 2, where for the TDNN-improved ephemerides, the estimated positions are 14-times better, and the estimated velocities are 3-times better than those obtained from TLE-initialized SGP4. During these last 5 minutes, a LEO receiver will localize itself by using an EKF that fuses Doppler measurements from the 19 satellites.

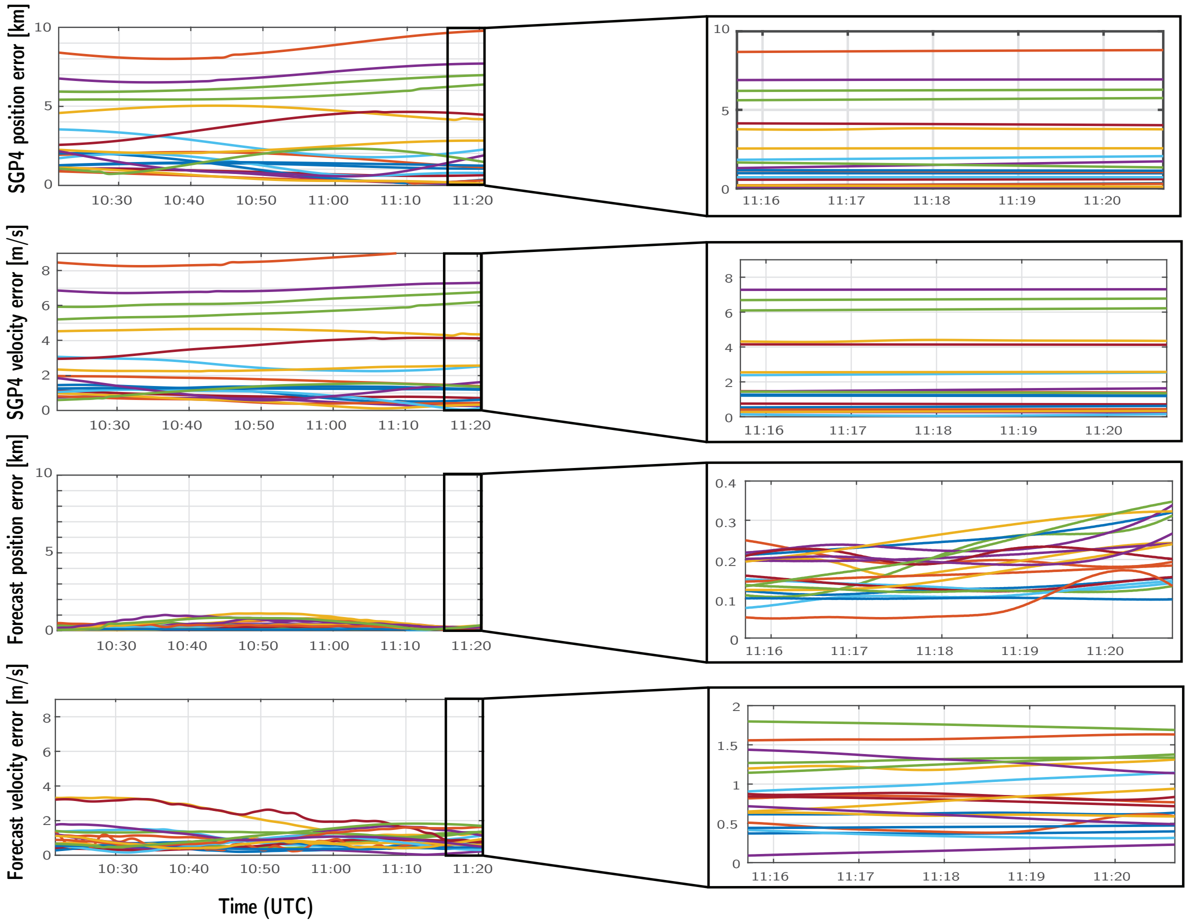

Figure 4: Satellites position and velocity errors of SGP4-propagated and TDNN-forcasted ephemerides. Each color represents one satellite.

Table 2: Mean satellite position and velocity errors of the SGP4-propagated and TDNN-corrected ephemerides

	Mean Position Error [m]	Mean Velocity Error [m/s]
SGP4	2,535	2.75
TDNN	177	0.86

2. Doppler Measurement Model

The LEO receiver extracted Doppler frequency measurements f_D from the Starlink satellites by subtracting the nominal carrier frequency from the received signal frequency. The pseudorange rate $\dot{\rho}$ is related to f_D by

$$\dot{\rho}(k) = -\frac{c}{f_c} f_D(k),$$

where f_c is the carrier frequency. At time-step k, the pseudorange rate can be modeled as

$$\dot{\rho}(k) = [\dot{\boldsymbol{r}}_{\mathrm{r}}(k) - \dot{\boldsymbol{r}}_{\mathrm{s}}(k)]^{\mathsf{T}} \frac{[\boldsymbol{r}_{\mathrm{r}}(k) - \boldsymbol{r}_{\mathrm{s}}(k')]}{\|\boldsymbol{r}_{\mathrm{r}}(k) - \boldsymbol{r}_{\mathrm{s}}(k')\|_2} + c \cdot [\dot{\delta} t_{\mathrm{r}}(k) - \dot{\delta} t_{\mathrm{s}}(k')] + c\delta t_{\mathrm{iono}}(k) + c\delta t_{\mathrm{tropo}}(k) + \upsilon_{\dot{\rho}}(k),$$

where $\boldsymbol{r}_\mathrm{r}$ and $\boldsymbol{r}_\mathrm{s}$ are the receiver's and the LEO satellite's 3D positions respectively; $\dot{\boldsymbol{r}}_\mathrm{r}$ and $\dot{\boldsymbol{r}}_\mathrm{s}$ are the receiver's and the LEO satellite's 3D velocities respectively; $\dot{\delta}t_\mathrm{r}$ and $\dot{\delta}t_\mathrm{s}$ are the receiver's and the satellite's clock drifts respectively; $\upsilon_{\dot{\rho}}$ is the pseudorange measurement noise, which is modeled as a zero-mean white Gaussian random sequence with variance $\sigma_{\dot{\rho}}^2(k)$; and k' is the discrete time at $t_{k'} = kT + t_0 - \delta t_\mathrm{TOF}$, with δt_TOF being the true time-of-flight (TOF) of the signal from the LEO satellite to the receiver. For simplicity, ionospheric $c\delta t_\mathrm{iono}$ and tropospheric $c\delta t_\mathrm{tropo}$ delay rate effects are assumed to be accounted for using models in the literature (Misra and Enge, 2010; Xu et al., 2023). The remaining modeling errors are lumped into the white measurement noise, with temporal correlations being ignore for simplicity. The Doppler measurements for all 19 satellites are shown in Figure 5.

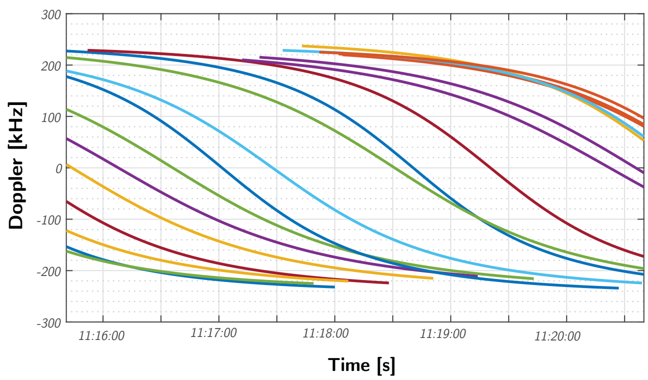

Figure 5: Simulated Doppler measurements from the 19 Starlink satellites

3. Localization Simulation

Now that the satellites' positions and velocities have been determined in three different ways: (i) ground truth data, retrieved directly from SpaceX ephemerides files; (ii) TLE and SGP4 propagation; and (iii) TDNN correction forecast; a stationary receiver was localized in Columbus, Ohio, USA by fusing the Doppler measurements via an EKF to estimate the state vector

$$\begin{aligned}
\boldsymbol{x}_\mathrm{r} &\triangleq [\boldsymbol{r}_\mathrm{r}^\mathsf{T}, c\Delta\delta t_1, c\Delta\dot{\delta}t_1, \ldots, c\Delta\delta t_n, c\Delta\dot{\delta}t_n] \\
c\Delta\delta t_l &= c\Delta\delta t_\mathrm{r} - c\Delta\delta t_{\mathrm{s},l} \\
c\Delta\dot{\delta}t_l &= c\Delta\dot{\delta}t_\mathrm{r} - c\Delta\dot{\delta}t_{\mathrm{s},l},
\end{aligned}$$

where $\boldsymbol{r}_\mathrm{r}$ represents the 3D position of the receiver, resolved in the Earth-centered, Earth-fixed (ECEF) frame and $c\Delta\delta t_l$ and $c\Delta\dot{\delta}t_l$ represent the relative clock bias and drift, respectively, between the receiver and the l-th LEO satellite l.

To generate representative localization results, 1,000 Monte Carlo realizations were conducted by randomizing the initial conditions around the true position of the receiver according to

$$\begin{aligned}
\hat{\boldsymbol{r}}(0|0) &\sim \mathcal{N}[\boldsymbol{r}_\mathrm{r}, \mathbf{P}_{\boldsymbol{r}_\mathrm{r}}(0|0)] \\
\mathbf{P}_{\boldsymbol{r}_\mathrm{r}}(0|0) &= \mathrm{diag}[10^7, 10^7, 10^7]\ \mathrm{m}^2.
\end{aligned}$$

In other words, the initial position estimates of the receiver were located randomly in a 99% confidence sphere of radius 9.5 km. Figure 6(a) shows the 1,000 initial estimates used in the simulation as red dots, while the blue pin represents the true receiver location. Figure 6(b) shows the EKF estimates using SGP4 ephemerides (red dots) and TDNN ephemerides (pink dots). It can be seen that the EKF using SGP4 ephemerides reduced the initial error; however, the estimates were inconsistent. This is attributed to ephemerides model mismatch. In contrast, the EKF using the TDNN ephemerides seemed to be consistent (spread out around the receiver's true location. Table 3 lists the average position error for: (i) best case scenario (using the ground truth SpaceX ephemerides), (ii) using the SGP4 propagator, and (iii) using the developed TDNN.

Table 3: Average initial and final position errors for the Monte Carlo simulation

	Initial Position Error [m]	**Final Position Error Error [m]**
Ground Truth	6,369	4
SGP4	6,369	2,305
TDNN	6,369	53

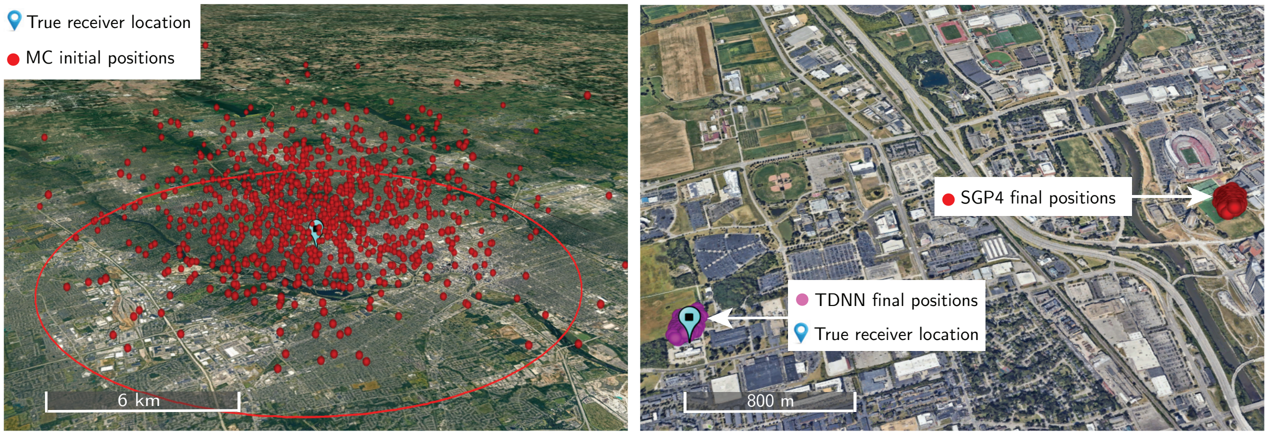

(a) Initial positions (b) Final position estimations

Figure 6: Final position estimations for TDNN and SGP4

V. CONCLUSION

This paper developed an ML framework for improved orbit prediction of Starlink LEO satellites. The framework is divided into two stages: (i) processing the data obtained from SpaceX ephemerides files and SGP4 propagator and training a TDNN on their difference and (ii) forecasting the errors for a certain time period to improve SGP4 propagation. The efficacy of the ML approach was demonstrated in a Doppler-based simulation with 19 Starlink LEO satellites by comparing the final localization errors of both SGP4 and TDNN approaches, starting with an initial position error of 6.5 km. For the SGP4, 1,000 Monte Carlo simulations resulted in an average localization error of 2.3 km error compared to 53 m with the TDNN.

ACKNOWLEDGMENTS

This work was supported in part by the Air Force Office of Scientific Research (AFOSR) under Grant FA9550-22-1-0476, in part by the National Science Foundation (NSF) under Grant 2240512, and in part by the U.S. Department of Transportation under Grant 69A3552348327 for the CARMEN+ University Transportation Center.

REFERENCES

Burbank, J., Greene, T., and Kaabouch, N. (2024). Detecting and mitigating attacks on GPS devices. *Sensors*, 24(17):1–47.

El-Mowafy, A., Wang, K., Li, Y., and Allahvirdi-Zadeh, A. (2023). The impact of orbital and clock errors on positioning from LEO constellations and proposed orbital solutions. *The International Archives of the Photogrammetry, Remote Sensing and Spatial Information Sciences*, 48:1111–1117.

Fan, G., Chen, X., Zhang, R., Wu, P., Wei, Q., Xu, W., Dai, J., and Cao, L. (2024). Toward massive satellite signals of opportunity positioning: Challenges, methods and experiments. *Space: Science & Technology*, pages 1–21.

Farhangian, F. and Landry, R. (2020). Multi-constellation software-defined receiver for Doppler positioning with LEO satellites. *Sensors*, 20(20):5866–5883.

Feng, F., Zhang, Y., Li, H., Fang, Y., Huang, Q., and Tao, X. (2019). A novel space-based orbit determination method based on distribution regression and its sparse solution. *IEEE Access*, 7:133203–133217.

Gal, Z. and Talbi, D. (2024). Insights into low Earth orbit satellite communication dynamics: quality of service analysis of connection behavior, latency, and Doppler shift. In *Proceedings of International Conference on Electronic Communications, Internet of Things and Big Data*, pages 116–121.

Gosalia, R., Malaney, R., Aguinaldo, R., Green, J., and Brereton, P. (2023). LEO clock synchronization with entangled light. In *Proceedings of IEEE Global Communications Conference*, pages 2317–2322.

Grayver, E., Nelson, R., McDonald, E., Sorensen, E., and Romano, S. (2024). Position and navigation using Starlink. In *Proceedings of IEEE Aerospace Conference*, pages 1–12.

Haidar-Ahmad, J., Khairallah, N., and Kassas, Z. (2022). A hybrid analytical-machine learning approach for LEO satellite orbit prediction. In *Proceedings of International Conference on Information Fusion*, pages 1–7.

Hartnett, M. (2022). Performance assessment of navigation using carrier Doppler measurements from multiple LEO constellations. Master's thesis, Air Force Institute of Technology, Ohio, USA.

Huang, C., Qin, H., Zhao, C., and Liang, H. (2022). Phase - time method: Accurate Doppler measurement for Iridium NEXT signals. *IEEE Transactions on Aerospace and Electronic Systems*, 58(6):5954–5962.

Imre, E. and Palmer, P. (2007). High-precision, symplectic numerical, relative orbit propagation. *Journal of Guidance, Control, and Dynamics*, 30:965–973.

Jardak, N. and Adam, R. (2023). Practical use of Starlink downlink tones for positioning. *Sensors*, 23(6):3234–3253.

Jardak, N. and Jault, Q. (2022). The potential of LEO satellite-based opportunistic navigation for high dynamic applications. *Sensors*, 22(7):2541–2565.

Kassas, Z., Hayek, S., and Haidar-Ahmad, J. (2024a). LEO satellite orbit prediction via closed-loop machine learning with application to opportunistic navigation. *IEEE Aerospace and Electronic Systems Magazine*. accepted.

Kassas, Z., Khairallah, N., and Kozhaya, S. (2024b). Ad astra: Simultaneous tracking and navigation with megaconstellation LEO satellites. *IEEE Aerospace and Electronic Systems Magazine*, 39(9):46–71.

Kassas, Z., Kozhaya, S., Kanj, H., Saroufim, J., Hayek, S., Neinavaie, M., Khairallah, N., and Khalife, J. (2023a). Navigation with multi-constellation LEO satellite signals of opportunity: Starlink, Oneweb, Orbcomm, and Iridium. In *Proceedings of IEEE/ION Position, Location, and Navigation Symposium*, pages 338–343.

Kassas, Z., Kozhaya, S., Saroufim, J., Kanj, H., and Hayek, S. (2023b). A look at the stars: Navigation with multi-constellation LEO satellite signals of opportunity. *Inside GNSS Magazine*, 18(4):38–47.

Kassas, Z., Neinavaie, M., Khalife, J., Khairallah, N., Haidar-Ahmad, J., Kozhaya, S., and Shadram, Z. (2021). Enter LEO on the GNSS stage: Navigation with Starlink satellites. *Inside GNSS Magazine*, 16(6):42–51.

Khairallah, N. and Kassas, Z. (2021). Ephemeris closed-loop tracking of LEO satellites with pseudorange and Doppler measurements. In *Proceedings of ION GNSS Conference*, pages 2544–2555.

Khalife, J. and Kassas, Z. (2019). Receiver design for Doppler positioning with LEO satellites. In *Proceedings of IEEE International Conference on Acoustics, Speech and Signal Processing*, pages 5506–5510.

Khalife, J., Neinavaie, M., and Kassas, Z. (2022). The first carrier phase tracking and positioning results with Starlink LEO satellite signals. *IEEE Transactions on Aerospace and Electronic Systems*, 56(2):1487–1491.

Kozhaya, S., Haidar-Ahmad, J., Abdallah, A., Kassas, Z., and Saab, S. (2021). Comparison of neural network architectures for simultaneous tracking and navigation with LEO satellites. In *Proceedings of ION GNSS Conference*, pages 2507–2520.

Kozhaya, S., Kanj, H., and Kassas, Z. (2023). Multi-constellation blind beacon estimation, Doppler tracking, and opportunistic positioning with OneWeb, Starlink, Iridium NEXT, and Orbcomm LEO satellites. In *Proceedings of IEEE/ION Position, Location, and Navigation Symposium*, pages 1184–1195.

Kozhaya, S., Saroufim, J., and Kassas, Z. (2024). Starlink for PNT: a trick or a treat? In *Proceedings of ION GNSS+ Conference*. accepted.

Lee, J. and Park, K. (2019). Gan-based imbalanced data intrusion detection system. *Personal and Ubiquitous Computing*, 25:121–128.

Liu, P., Voon Ling, K., Qin, H., Jiang, M., and Lu, J. (2024). Actualization analysis of LEO opportunistic doppler aided GNSS precise point positioning using moving horizon estimation. *IEEE Transactions on Vehicular Technology*, pages 1–12. accepted.

Misra, P. and Enge, P. (2010). *Global Positioning System: Signals, Measurements, and Performance*. Ganga-Jamuna Press, second edition.

Montenbruck, O. and Gill, E. (2000). *Satellite orbits: models, methods, and applications*. Springer.

Morales, J., Khalife, J., Santa Cruz, U., and Kassas, Z. (2019). Orbit modeling for simultaneous tracking and navigation using LEO satellite signals. In *Proceedings of ION GNSS Conference*, pages 2090–2099.

Mortlock, T. and Kassas, Z. (2021). Assessing machine learning for LEO satellite orbit determination in simultaneous tracking and navigation. In *Proceedings of IEEE Aerospace Conference*, pages 1–8.

North American Aerospace Defense Command (NORAD) (2018). Two-line element sets. `http://celestrak.com/NORAD/elements/`.

Peng, H. and Bai, X. (2017). Limits of machine learning approach on improving orbit prediction accuracy using support vector machine. In *Proceedings of Advanced Maui Optical and Space Surveillance Technologies Conference*, pages 1–22.

Peng, H. and Bai, X. (2018). Artificial neural network–based machine learning approach to improve orbit prediction accuracy. *Journal of Spacecraft and Rockets*, 55(5):1248–1260.

Peng, H. and Bai, X. (2019). Comparative evaluation of three machine learning algorithms on improving orbit prediction accuracy. *Astrodynamics*, 3(4):325–343.

Prol, F., Bhuiyan, M., Kaasalainen, S., Lohan, S., Praks, J., Celikbilek, K., and Kuusniemi, H. (2024). Simulations of dedicated LEO-PNT systems for precise point positioning: Methodology, parameter analysis, and accuracy evaluation. *IEEE Transactions on Aerospace and Electronic Systems*, pages 1–19. accepted.

Reid, T., Walter, T., Enge, P., Lawrence, D., Cobb, H., Gutt, G., O'Conner, M., and Whelan, D. (2021). Position, navigation, and timing technologies in the 21st century. volume 2, chapter 43: Navigation from low Earth orbit – Part 1: concept, current capability, and future promise, pages 1359–1379. Wiley-IEEE.

Salleh, N., Yuhaniz, S., Azmi, N., and Sabri, S. (2019). Enhancing simplified general perturbations-4 model for orbit propagation using deep learning: A review. In *Proceedings of the International Conference on Software and Computer Applications*, pages 27–32.

Schutz, B., Tapley, B., and Born, G. (2004). *Statistical orbit determination*. Elsevier.

Shahcheraghi, S. and Kassas, Z. (2024). A computationally efficient approach for acquisition and Doppler tracking for PNT with LEO megaconstellations. *IEEE Signal Processing Letters*, 31:2400–2404.

Sharma, S. and Cutler, J. (2015). Robust orbit determination and classification: A learning theoretic approach. *IPN Progress Report*, pages 42–203.

Shen, S., Sheaff, C., Guo, M., Blasch, E., Pham, K., and Chen, G. (2021). Three-dimensional convolutional neural network (3D-CNN) for satellite behavior discovery. In *Proceedings of SPIE Sensors and Systems for Space Applications*, volume 11755, pages 1–18.

Starlink (2024). Starlink ephemerides. `https://www.space-track.org/`.

Stock, W., Schwarz, R., Hofmann, C., and Knopp, A. (2024). Survey on opportunistic PNT with signals from LEO communication satellites. *IEEE Communications Surveys & Tutorials*, pages 1–31. accepted.

Tan, Z., Qin, H., Cong, L., and Zhao, C. (2019). New method for positioning using IRIDIUM satellite signals of opportunity. *IEEE Access*, 7:83412–83423.

Union of Concerned Scientists (2024). UCS satellite database. `https://www.ucsusa.org/resources/satellite-database`.

Wang, D., Qin, H., Liang, H., and Zhang, Y. (2024). Clock error analysis and compensation for LEO signal of opportunity positioning. *IEEE Sensors Journal*, 24(8):12716–12727.

Wang, Y., Bai, X., Peng, H., Chen, G., Shen, D., Blasch, E., and Sheaff, C. (2021). Gaussian-binary classification for resident space object maneuver detection. *Acta Astronautica*, 187:438–446.

Xie, W., Su, H., Wang, K., Liu, J., Wi, M., andA. El-Mowafy, M. Z., and Yang, X. (2024a). Real-time LEO satellite clock estimation with predicted LEO satellite orbits constrained. *GPS Solutions*, 28.

Xie, Y., Li, G., Qin, H., Zhao, C., Chen, M., and Zhou, W. (2024b). Carrier phase tracking and positioning algorithm with additional system parameters based on Orbcomm signals. *GPS Solutions*, 28(4):1–17.

Xu, J., Morton, Y., Xu, D., Jiao, Y., and Hinks, J. (2023). Tracking GNSS-like signals transmitted from LEO satellites and propagated through ionospheric plasma irregularities. In *Proceedings of ION GNSS+ Conference*, pages 2813–2822.

Ye, L., Gao, N., Yang, Y., Deng, L., and Li, H. (2023). Three satellites dynamic switching range integrated navigation and positioning algorithm with clock bias cancellation and altimeter assistance. *Aerospace*, 10(5):411–438.

Zeroual, A., Harrou, F., Dairi, A., and Sun, Y. (2020). Deep learning methods for forecasting COVID-19 time-series data: A comparative study. *Chaos, Solitons and Fractals*, 140:110–121.

Zhao, C., Qin, H., Wu, N., and Wang, D. (2023). Analysis of baseline impact on differential Doppler positioning and performance improvement method for LEO opportunistic navigation. *IEEE Transactions on Instrumentation and Measurement*, 72:1–10.